Global Analysis of a Dynamic Duopoly Game with Bounded Rationality

Gian Italo Bischi
Istituto di Scienze Economiche
Università di Urbino
Urbino, Italy

Ahmad Naimzada
Università "L. Bocconi"
Milano, Italy

Abstract

A dynamic Cournot duopoly game, characterized by firms with bounded rationality, is represented by a discrete-time dynamical system of the plane. Conditions ensuring the local stability of a Nash equilibrium, under a local (or myopic) adjustment process, are given, and the influence of marginal costs and speeds of adjustment of the two firms on stability is studied. The stability loss of the Nash equilibrium, as some parameter of the model is varied, gives rise to more complex (periodic or chaotic) attractors. The main result of this paper is given by the exact determination of the basin of attraction of the locally stable Nash equilibrium (or other more complex bounded attractors around it), and the study of the global bifurcations that change the structure of the basin from a simple to a very complex one, with consequent loss of predictability, as some parameters of the model are allowed to vary. These bifurcations are studied by the use of critical curves, a relatively new and powerful method for the study of noninvertible two-dimensional maps.

1   Introduction

The static Cournot oligopoly model, in which each firm, given the optimal production decisions of the other firms selling the same homogeneous good, sets its optimal production, is a fully rational game based on the following assumptions:

(i) each firm, in taking its optimal production decision, must know beforehand all its rivals' production decisions taken at the same time;

(ii) each firm has a complete knowledge of the market demand function.

Under these conditions of full information the system moves straight (in one shot) to a Nash equilibrium, if it exists, independently of the initial status of the market, so that no dynamic adjustment process is needed. Dynamic Cournot oligopoly models arise from more plausible assumptions of partial information, so that the

players' behavior is not fully rational. For example, a dynamic model is obtained if assumption (i) is replaced by some kind of expectation on the rivals' outputs. The simplest kind of expectation, based on Cournot's assumption that each firm, in taking its optimal decision, guesses that the output of the other firms remains at the same level as in the previous period, has given rise to a flourishing literature on dynamic oligopoly models, starting from the seminal paper of Teocharis [18] (see, e.g., McManus and Quandt [11], Fisher [6], Hahn [10], and Okuguchi [15]).

Models where also assumption (ii) is relaxed have recently been proposed by many authors, e.g., Bonanno and Zeeman [3], Bonanno [2], and Sacco [16]. In these models firms are supposed to have a knowledge of demand function limited to a small neighborhood of the status of the market in which they operate, and use such local knowledge to update their production strategy by a local profit maximization. Since they play the game repeatedly, they can gradually adjust their production over time. In these dynamic models a Nash equilibrium, if it exists, is a stationary state, i.e., if all the firms have outputs at the Nash equilibrium, their production decisions will remain the same forever. Instead, if the oligopoly system is outside a Nash equilibrium, then the repeated local adjustment process may converge to the Nash equilibrium, where there is no further possibility for improvement, or may move around it by a periodic or aperiodic time evolution, or may irreversibly depart from it. Thus the main question addressed in the literature on dynamic oligopoly models is that of the stability of the Nash equilibria, and how such stability is influenced by the model structure and the values of the parameters which characterize the model. Results of global asymptotic stability, which means that the adjustment process converges to the Nash equilibrium independently of the initial condition, have been given both for linear models, by the analysis of the eigenvalues of the model, and for nonlinear models by the second Lyapunov method, as in Rosen [17]. On the contrary, the question of stability extent in models, in which global stability does not hold, has been rather neglected in the literature. In fact, for nonlinear models, the analysis is often limited to the study of the linear approximation, but these results are in general quite unsatisfactory for practical purposes, since they determine the attractivity of a Nash equilibrium only for games starting in some region around the equilibrium, and such a region may be so small that every practical meaning of the mathematical concept of stability is lost. In these cases the question of the stability extent, that is, the delimitation of the basin of attraction of a locally stable equilibrium, becomes crucial for any practical stability result. In fact, only an exact determination of the boundaries of the basin of attraction can give a clear idea of the robustness of an attractor with respect to exogenous perturbations, always present in real systems, since it permits one to understand if a given shock of finite amplitude can be recovered by the endogenous dynamics of the system, or if it will cause an irreversible departure from the Nash equilibrium.

The present paper moves toward this less explored direction. We propose a nonlinear, discrete-time, duopoly model, where a Nash equilibrium exists that is,

under given conditions on the model's parameters, locally asymptotically stable, but not globally stable.

The adjustment mechanism considered in this paper is based on the pseudo-gradient of the profit functions, i.e., each player changes its own production so as to obtain the maximum rate of change of its own profit with respect to a change in its own strategy. Such an adjustment has been proposed, in a continuous time model, by Rosen [17], and similar mechanisms are also considered by Furth [8], Sacco [16], Varian [19], and Flam [7]. In the paper by Rosen it is shown that, under the assumption of strict diagonal concavity of the payoffs, the unique equilibrium is globally asymptotically stable. In this paper we show that if a discrete-time model is considered the situation is more complex, since even if the conditions for stability required by Rosen are satisfied, local stability does not imply global stability.

The plan of the paper is as follows. A detailed description of the model is given in Section 2. In Section 3 the existence and local stability of the equilibrium points of the model are studied. The main results of the paper are given in Section 4, where the exact delimitation of the basin of attraction of the Nash equilibrium is obtained. The occurrence, as some parameter is allowed to vary, of some global bifurcations causing qualitative changes in the structure of the basins is studied by the use of critical curves, a powerful tool for the analysis of noninvertible maps of the plane. In this section we also show that even when the Nash equilibrium becomes unstable, the process may be characterized by periodic or chaotic trajectories which are confined in a bounded region around the Nash equilibrium, so that the duopoly system continues to have an asymptotic behavior which is not far from optimality. In any case, the global analysis of the dynamical system reveals that bifurcations can occur, as some parameter is left to vary, that cause qualitative changes in the structure of the basins of attraction.

2   The Duopoly Model: Assumptions and Notations

We consider an industry consisting of two quantity-setting firms, labeled by $i = 1, 2$, producing the same good for sale on the market. Production decisions of both firms occur at discrete-time periods $t = 0, 1, 2, ...$ Let $q_i(t)$ represent the output of the ith firm during period t, at a production cost $C_i(q_i)$. The price prevailing in period t is determined by the total supply $Q(t) = q_1(t) + q_2(t)$ through a demand function

$$p = f(Q) \tag{1}$$

from which the single-period profit of ith firm is given by

$$\Pi_i(q_1, q_2) = q_i f(Q) - C_i(q_i). \tag{2}$$

As stressed in Section 1, we assume that each duopolist does not have a complete knowledge of the demand function, and tries to infer how the market will respond

to its production changes by an empirical estimate of the marginal profit. This estimate may be obtained by market research or by brief experiments of small (or local) production variations performed at the beginning of period t (see Varian [19]) and we assume that even if the firms are quite ignorant about the market demand, they are able to obtain a correct empirical estimate of the marginal profits, i.e.,

$$\Phi_i(t) = \left(\frac{\partial \Pi_i}{\partial q_i}\right)^{(e)} = \frac{\partial \Pi_i}{\partial q_i}(q_1, q_2), \qquad i = 1, 2. \tag{3}$$

Of course, this local estimate of expected marginal profits is much easier to obtain than a global knowledge of the demand function (involving values of Q that may be very different from the current ones). With this kind of information the producers behave as local profit maximizers, the local adjustment process being one where a firm increases its output if it perceives a positive marginal profit $\Phi_i(t)$, and decreases its production if the perceived $\Phi_i(t)$ is negative. This adjustment mechanism has been called by some authors *myopic* (see Dixit [5] and Flam [7]). Let $G_i(\cdot)$, $i = 1, 2$, be an increasing function, such that

$$\operatorname{sgn} G_i(\cdot) = \operatorname{sgn}(\cdot), \qquad i = 1, 2. \tag{4}$$

Then the dynamic adjustment mechanism can be modeled as

$$q_i(t + 1) = q_i(t) + \alpha_i(q_i) G_i(\Phi_i), \qquad i = 1, 2, \tag{5}$$

where $\alpha_i(q_i)$ is a positive function which gives the extent of production variation of the ith firm following a given profit signal Φ_i. It is important to note that a Nash equilibrium, if it exists, is also a fixed point of the dynamical system (5). In fact, a Nash equilibrium is located at the intersection of the reaction curves, defined by $(\partial \Pi_i/\partial q_i)(q_1, q_2) = 0$, $i = 1, 2$ (as noticed by Dixit [5], the term "reaction curve" is not appropriate in models like (5), since they describe a simultaneous-move game, but we follow the tradition of using the same term also in this context). Since (4) implies $G_i(0) = 0$, $i = 1, 2$, the dynamic process (5) is stationary if the strategy point (q_1, q_2) is at a Nash equilibrium. The converse is not necessarily true, that is, stationary points of (5) that are not Nash equilibria can exist, as we shall see in the particular model studied in the following.

An adjustment mechanism similar to (5) has been proposed by some authors, mainly with continuous time and constant α_i (see, e.g., Rosen [17], Furth [8], Sacco [16], Varian [19], and Flam [7]). However, we believe that a discrete-time decision process is more realistic since in real economic systems production decisions cannot be revised at every time instant. We also assume that α_i are increasing functions of q_i (hence of the "size" of the firm). This assumption captures the fact that in the presence of a positive profit signal $\Phi_i > 0$, a bigger firm has greater capacity to make investments in order to increase its production, whereas in the presence of a negative profit signal a bigger producer must reduce more drastically its production to avoid bankruptcy risks.

In the following we shall assume, for sake of simplicity, a linear relation

$$\alpha_i(q_i) = v_i q_i, \qquad i = 1, 2, \tag{6}$$

where v_i is a positive constant that will be called *speed of adjustment*. We also assume a linear demand function

$$f(Q) = a - bQ \tag{7}$$

with a, b positive constants, and linear cost functions

$$C_i(q_i) = c_i q_i, \qquad i = 1, 2, \tag{8}$$

where the positive constants c_i are the marginal costs. With these assumptions

$$\Pi_i(q_1, q_2) = q_i \left[a - b(q_1 + q_2) - c_i \right], \qquad i = 1, 2, \tag{9}$$

and the marginal profit for firm i at the point (q_1, q_2) of the strategy space is

$$\Phi_i = \frac{\partial \Pi_i}{\partial q_i} = a - c_i - 2bq_i - bq_j, \qquad i, j = 1, 2, \quad j \neq i. \tag{10}$$

If, as in the quoted papers of Varian, Furth, Flam, and Sacco we consider a linear adjustment function

$$G(\Phi) = \Phi \tag{11}$$

the model (5), with the above assumptions, gives rise to the following two-dimensional nonlinear map $T(q_1, q_2) \rightarrow (q_1', q_2')$ defined as

$$T : \begin{cases} q_1' = (1 + v_1(a - c_1))q_1 - 2bv_1 q_1^2 - bv_1 q_1 q_2, \\[2mm] q_2' = (1 + v_2(a - c_2))q_2 - 2bv_2 q_2^2 - bv_2 q_1 q_2, \end{cases} \tag{12}$$

where $'$ denotes the unit-time advancement operator, that is, if the right-hand side variables are productions of period t, then the left-hand ones represent productions of period $(t + 1)$.

The map (12) is a noninvertible map of the plane, that is, starting from some nonnegative initial production strategy

$$(q_{1_0}, q_{2_0}) \tag{13}$$

the iteration of (12) uniquely defines the trajectory $(q_1(t), q_2(t)) = T^t(q_{1_0}, q_{2_0})$, $t = 1, 2, ...$, whereas the backward iteration of (12) is not uniquely defined. In fact, a point (q_1', q_2') of the plane may have several preimages, obtained by solving the fourth-degree algebraic system (12) with respect to q_1 and q_2 (see Mira et al. [12] for a complete treatment of the properties of noninvertible maps of the plane). The study of the dynamical properties of (12) allows us to have information on the long-run behavior of a bounded rationality adjustment process starting from a given initial condition (13), and how this is influenced by the parameters of the model.

3   Equilibrium Points and Local Stability

We define *equilibrium point* (or *stationary point*) of the dynamic duopoly game as a nonnegative fixed point of the map (12), i.e., a solution of the algebraic system

$$\begin{cases} q_1(a - c_1 - 2bq_1 - bq_2) = 0, \\ q_2(a - c_2 - bq_1 - 2bq_2) = 0, \end{cases} \tag{14}$$

obtained by setting $q_i' = q_i$, $i = 1, 2$, in (12). We can have at most four fixed points: $E_0 = (0, 0)$, $E_1 = [(a - c_1)/2b, 0]$ if $c_1 < a$, $E_2 = [0, (a - c_2)/2b]$ if $c_2 < a$, which will be called *boundary equilibria*, and the fixed point $E_* = (q_1^*, q_2^*)$, with

$$q_1^* = \frac{a + c_2 - 2c_1}{3b}, \qquad q_2^* = \frac{a + c_1 - 2c_2}{3b}, \tag{15}$$

provided that

$$\begin{cases} 2c_1 - c_2 < a, \\ 2c_2 - c_1 < a. \end{cases} \tag{16}$$

It is easy to verify that the equilibrium point E_*, when it exists, is the unique Nash equilibrium, located at the intersection of the two reaction curves given by the two straight lines which represent the locus of points of vanishing marginal profits (10). In the following we shall assume that (16) are satisfied, so that the Nash equilibrium E_* exists.

An important feature of the map (12) is that it can generate unbounded (i.e., divergent) trajectories (this can also be expressed by saying that (12) has an attracting set at infinite distance). In fact, unbounded (and negative) trajectories are obtained if the initial condition (13) is taken sufficiently far from the origin, i.e., in a suitable neighborhood of infinity, since if $q_{i0} > (1 + a - c_i)/bv_i$, $i = 1, 2$, then the first iterate of (12) gives negative values $q_i' < 0$, $i = 1, 2$, so that the successive iterates give negative and decreasing values because $q_i' = q_i + v_i q_i (a - c_i - 2bq_i - bq_j) < q_i$ being $(a - c_i) > 0$ if (16) hold. This implies that any attractor at finite distance cannot be globally attracting in $\mathbb{R}_+^2$, since its basin of attraction cannot extend out of the rectangle $[0, (1 + a - c_1)/bv_1] \times [0, (1 + a - c_2)/bv_2]$.

The study of the local stability of the fixed points is based on the localization, on the complex plane, of the eigenvalues of the Jacobian matrix of (12)

$$J(q_1, q_2) = \begin{bmatrix} 1 + v_1(a - c_1 - 4bq_1 - bq_2) & -v_1 bq_1 \\ -v_2 bq_2 & 1 + v_2(a - c_2 - bq_1 - 4bq_2) \end{bmatrix}. \tag{17}$$

It is easy to prove that whenever the equilibrium E_* exists (i.e., (16) are satisfied), the boundary fixed points E_i, $i = 0, 1, 2$, are unstable. In fact, at E_0 the Jacobian

matrix becomes a diagonal matrix

$$J(0, 0) = \begin{bmatrix} 1 + v_1(a - c_1) & 0 \\ 0 & 1 + v_2(a - c_2) \end{bmatrix}, \tag{18}$$

whose eigenvalues, given by the diagonal entries, are greater than 1 if $c_1 < a$ and $c_2 < a$. Thus E_0 is a repelling node with eigendirections along the coordinate axes. At E_1 the Jacobian matrix becomes a triangular matrix

$$J\left(\frac{a - c_1}{2b}, 0\right) = \begin{bmatrix} 1 - v_1(a - c_1) & -(v_1/2)(a - c_1) \\ 0 & 1 + (v_2/2)(a - 2c_2 + c_1) \end{bmatrix} \tag{19}$$

whose eigenvalues, given by the diagonal entries, are $\lambda_1 = 1 - v_1(a - c_1)$, with eigenvector $r_1^{(1)} = (1, 0)$ along the q_1-axis, and $\lambda_2 = 1 + (v_2/2)(a - 2c_2 + c_1)$, with eigenvector $r_1^{(2)} = (1, 2[1 - v_1(a - c_1)]/v_1(a - c_1))$. When (16) are satisfied E_1 is a saddle point, with local stable manifold along the q_1-axis and the unstable one tangent to $r_1^{(2)}$, if

$$v_1 < \frac{2}{a - c_1}, \tag{20}$$

otherwise E_1 is an unstable node. The bifurcation occurring at $v_1 = 2/(a - c_1)$ is a flip bifurcation at which E_1 from attracting becomes repelling along the q_1-axis, on which a saddle cycle of period 2 appears.

The same arguments hold for the other boundary fixed point E_2. It is a saddle, with local stable manifold along the q_2-axis and the unstable one tangent to $r_2^{(2)} = (1, 2[1 - v_2(a - c_2)]/v_2(a - c_2))$, if

$$v_2 < \frac{2}{a - c_2}, \tag{21}$$

otherwise it is an unstable node. Also, in this case, the bifurcation that transforms the saddle into the repelling node is a flip bifurcation creating a 2-cycle saddle on the q_2-axis.

To study the local stability of the Nash equilibrium we consider the Jacobian matrix at E_*

$$J(q_1^*, q_2^*) = \begin{bmatrix} 1 - 2v_1bq_1^* & -v_1bq_1^* \\ -v_2bq_2^* & 1 - 2v_2bq_2^* \end{bmatrix}. \tag{22}$$

Its eigenvalues are real because the characteristic equation $\lambda^2 - \text{Tr}\,\lambda + \text{Det} = 0$, where Tr represents the trace and Det the determinant of (22), has positive discriminant

$$\text{Tr}^2 - 4\,\text{Det} = 4b^2\left[\left(v_1q_1^* - v_2q_2^*\right)^2 + v_1v_2q_1^*q_2^*\right] > 0.$$

It is easy to realize that $\lambda_i < 1$, $i = 1, 2$, since $1 - \text{Tr} + \text{Det} > 0$ when (16) hold, thus a sufficient condition for the local asymptotic stability of E_* is
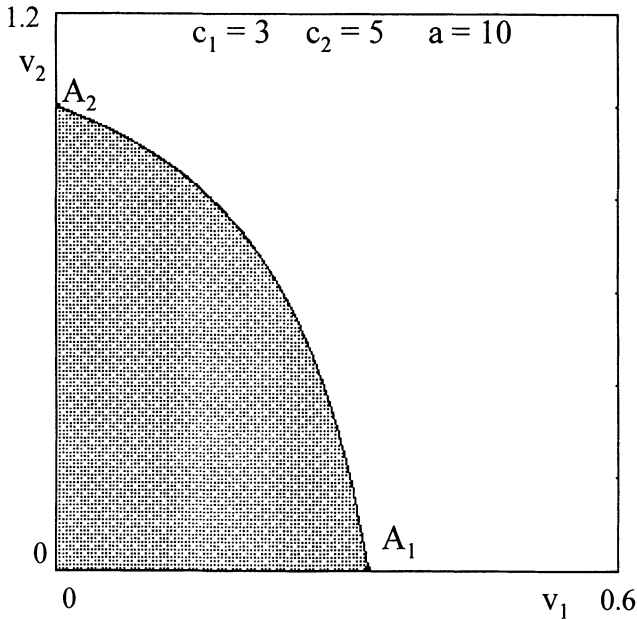
Figure 1: The shaded area represents, in the plane of speeds of adjustment (v_1, v_2), the region of local asymptotic stability of the Nash equilibrium. The values of the other parameters are $c_1 = 3$, $c_2 = 5$, $a = 10$.

$1 + \text{Tr} + \text{Det} > 0$, which ensures $\lambda_i > -1$, $i = 1, 2$ (see, e.g., Gumowski and Mira [9, p. 159]). This condition, which becomes

$$3b^2 q_1^* q_2^* v_1 v_2 - 4bq_1^* v_1 - 4bq_2^* v_2 + 4 < 0, \tag{23}$$

defines a region of stability in the plane of the speeds of adjustment (v_1, v_2) whose shape is like the shaded area of Figure 1. This stability region is bounded by the portion of hyperbola, with positive v_1 and v_2, whose equation is given by the vanishing of the left-hand side of (23). For values of (v_1, v_2) inside the stability region the Nash equilibrium E_* is a stable node, and the hyperbola represents a bifurcation curve at which E_* looses its stability through a period doubling (or *flip*) bifurcation. This bifurcation curve intersects the axes v_1 and v_2 in the points A_1 and A_2, respectively, whose coordinates are given by

$$A_1 = \left(\frac{3}{a + c_2 - 2c_1}, 0 \right) \quad \text{and} \quad A_2 = \left(0, \frac{3}{a + c_1 - 2c_2} \right). \tag{24}$$

From these results we can obtain information on the effects of the model's parameters on the local stability of E_*. For example, an increase of the speeds of adjustment, with the other parameters held fixed, has a destabilizing effect. In fact, an increase of v_1 and/or v_2, starting from a set of parameters which ensures the local stability of the Nash equilibrium, can bring the point (v_1, v_2) out of the

stability region, crossing the flip bifurcation curve. This destabilizing effect has already been evidenced by many authors (see, e.g., Fisher [6] and Flam [7]).

Similar arguments apply if the parameters v_1, v_2, c_1, c_2 are fixed and the parameter a, which represents the maximum price of the good produced, is increased. In this case, the stability region becomes smaller, as can easily be deduced from (24), and this can cause a loss of stability of E_* when the moving boundary is crossed by the point (v_1, v_2). An increase of the marginal cost c_1, with c_2 held fixed, causes a displacement of the point A_1 to the right and of A_2 downward. Instead, an increase of c_2, with c_1 held fixed, causes a displacement of A_1 to the left and of A_2 upward. In both cases the effect on the local stability of E_* depends on the position of the point (v_1, v_2). In fact, if $v_1 < v_2$, i.e., the point (v_1, v_2) is above the diagonal $v_1 = v_2$, an increase of c_1 can destabilize E_*, whereas an increase of c_2 reinforces its stability. The situation is reversed if $v_1 > v_2$.

From these arguments the combined effects due to simultaneous changes of more parameters can be deduced. For example, if E_* becomes unstable because of a price increase (due to a shift of the demand curve), its stability can be regained by a reduction of the speeds of reaction, whereas an increase of a marginal cost c_i can be compensated for by a decrease of the corresponding v_i, i.e., in the presence of a high marginal cost stability is favored by a more prudent behavior (i.e., lower reactivity to profit signals).

Another important property of the map (12) is that each coordinate axis $q_i = 0$, $i = 1, 2$, is trapping, that is, mapped into itself, since $q_i = 0$ gives $q'_i = 0$ in (12). This means that starting from an initial condition on a coordinate axis (*monopoly case*) the dynamics is confined in the same axis for each t, governed by the restriction of the map T to that axis. Such a restriction is given by the following one-dimensional map, obtained from (12) with $q_i = 0$

$$q_j = f_j(q_j) = (1 + v_j(a - c_j))q_j - 2bv_jq_j^2, \qquad j = 1, 2, \quad j \neq i. \qquad (25)$$

This map is conjugate to the standard logistic map

$$x' = \mu x (1 - x) \qquad (26)$$

through the linear transformation

$$q_j = \frac{1 + v_j(a - c_j)}{2bv_j}x \qquad (27)$$

from which we obtain the relation

$$\mu = 1 + v_j(a - c_j). \qquad (28)$$

This means that the dynamics of (25) can be obtained from the well-known dynamics of (26). A brief description of the main features of the map (25) is given in Appendix B, because the dynamic behavior of the restrictions of T to the invariant axes plays an important role in the understanding of the global properties of the duopoly model.

4 Basin Boundaries and Their Bifurcations

In Section 3 we have shown that if the conditions (16) are satisfied then the Nash equilibrium $E_* = (q_1^*, q_2^*)$ exists, and it is locally asymptotically stable provided that (23) holds true. In this section we consider the question of the stability extent of the Nash equilibrium, or of different bounded attracting sets around it. In the following we call *attractor at finite distance*, denoted by $\mathcal{A}$, a bounded attracting set (which may be the Nash equilibrium E_*, a periodic cycle, or some more complex attractor around E_*) in order to distinguish it from the limit sets at infinite distance, i.e., the unbounded trajectories, which represent exploding (or collapsing) evolutions of the duopoly system. We denote by $\mathcal{D}(\mathcal{A})$ the basin of attraction of an attractor $\mathcal{A}$, defined as the open set of points (q_1, q_2) of the phase plane whose trajectories $T'(q_1, q_2)$ have limit sets belonging to $\mathcal{A}$ as $t \rightarrow +\infty$. We also denote by $\mathcal{D}(\infty)$ the *basin of infinity*, defined as the set of points which generate unbounded trajectories. Let $\mathcal{F}$ be the boundary (or frontier) separating $\mathcal{D}(\mathcal{A})$ from $\mathcal{D}(\infty)$. An exact determination of $\mathcal{F}$ is the main goal of this section. Indeed, this boundary may be rather complex, as evidenced by the numerical results shown in Figure 2. In Figure 2(a) the attractor at finite distance is the Nash equilibrium E_*, and its basin of attraction is represented by the white area, whereas the grey-shaded area represents the basin of infinity. Two typical trajectories are also shown in Figure 2(a), one converging to E_* and one divergent. Notice that in Figure 2(a) the adjustment process which starts from the grey region, and consequently exhibits an irreversible departure from the Nash equilibrium, starts from an initial production strategy which is closer to the Nash equilibrium than the convergent one, a rather counterintuitive result. In the situation shown in Figure 2(a), the boundary separating $\mathcal{D}(\mathcal{A})$ from $\mathcal{D}(\infty)$ has a fractal boundary, as will be explained below. In Figure 2(b) the bounded attractor $\mathcal{A}$ is a chaotic set, with a multiply connected (or connected with holes) basin of attraction. The same property can be expressed by saying that $\mathcal{D}(\infty)$ is a nonconnected set, with nonconnected regions given by the holes inside $\mathcal{D}(\mathcal{A})$ (see Mira et al. [12] or Mira et al. [13]). In this situation there is a great uncertainty about the long-run behavior of a given adjustment process, since a small change in the initial strategy of the game may cause a crossing of $\mathcal{F}$.

4.1 Determination of the Basin Boundaries

The boundary $\mathcal{F} = \partial \mathcal{D}(\mathcal{A}) = \partial \mathcal{D}(\infty)$ behaves as a repelling line for the points near it, since it acts as a watershed for the trajectories of the map T. Points belonging to $\mathcal{F}$ are mapped into $\mathcal{F}$ both under forward and backward iteration of T, that is, the boundary is invariant for application of T and T^{-1}. More exactly $T(\mathcal{F}) \subseteq \mathcal{F}$, $T^{-1}(\mathcal{F}) = \mathcal{F}$ (see Mira et al. [12] and Mira and Rauzy [14]). This implies that if a saddle point, or a saddle cycle, belongs to $\mathcal{F}$, then $\mathcal{F}$ must also contain all the preimages of such singularities, and it must also contain the whole stable
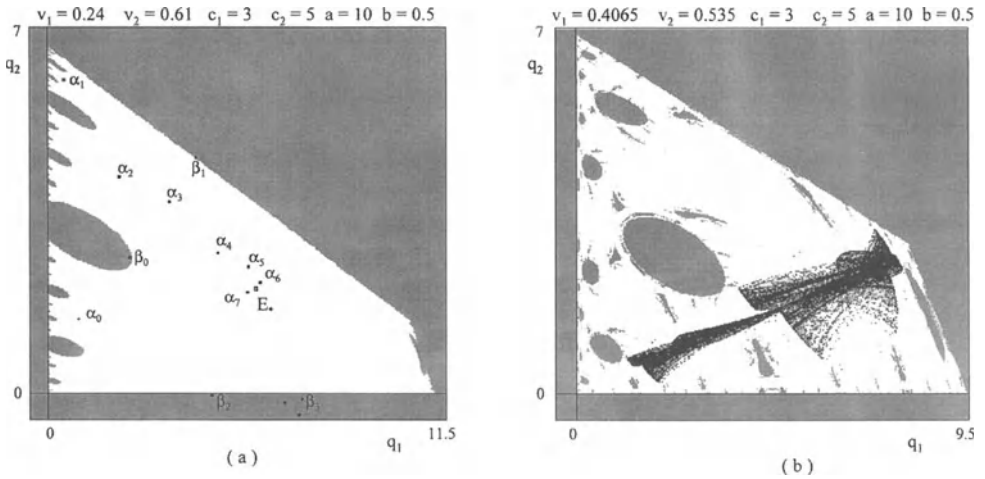
Figure 2: Numerical representation of the basins of attraction for the duopoly map. The two figures are obtained by taking a grid of initial conditions (q_{10}, q_{20}) and generating, for each of them, a numerically computed trajectory of the duopoly map. If the trajectory is diverging (i.e., if it reaches large negative values) then a grey dot is painted in the point corresponding to the initial condition, otherwise a white dot is painted. In Figure **(a)** the white region represents the basin of attraction of the Nash equilibrium, which is the only attractor at finite distance for that set of parameters. In this figure also the early points of two typical trajectories, one convergent to E_*, denoted by $\{\alpha_0, \alpha_1, ...\}$, and one divergent, denoted by $\{\beta_0, \beta_1, ...\}$,are represented. In Figure **(b)** the attractor at finite distance is given by a chaotic attractor surrounding the unstable Nash equilibrium.

manifold W^s (see Gumowski and Mira [9] and Mira et al. [13]). For example, the saddle fixed points (or the saddle cycles, if (20) or (21) no longer hold) located on the coordinate axes belong to $\mathcal{F}$, and also the invariant coordinate axes, which form the local stable manifold (or inset) of the saddles, are part of $\mathcal{F}$.

Let us consider the two segments $\omega_j = \left[0, 0^{(j)}_{-1}\right]$, where $0^{(j)}_{-1}$, $j = 1, 2$, is the rank-1 preimage of the origin computed according to the restriction (25), i.e.,

$$0^{(j)}_{-1} = \frac{1 + v_j (a - c_j)}{2bv_j}, \qquad j = 1, 2. \tag{29}$$

Instead, negatively divergent trajectories along the invariant axis q_j are obtained starting from an initial condition out of the segment ω_j. The segments ω_1 and ω_2 on the two coordinate axes play an important role in the determination of $\mathcal{F}$. In fact:

(a) from the computation of the eigenvalues of the cycles belonging to ω_1 and ω_2 we have that the direction transverse to the coordinate axes is always repelling; and

(b) a point $\left(q_{1_0}, q_{2_0}\right)$ generates a divergent trajectory if $q_{1_0} < 0$ or $q_{2_0} < 0$.

From (a) and (b) it follows that ω_1 and ω_2 belong to $\mathcal{F}$, as well as their preimages of any rank. From these arguments the following proposition can be stated, that gives an exact determination of $\mathcal{F}$.

Proposition 4.1. *Let* $\omega_1 = \left[0, 0_{-1}^{(1)}\right]$ *and* $\omega_2 = \left[0, 0_{-1}^{(2)}\right]$ *be the segments of the coordinate axes* q_1 *and* q_2, *respectively, with* $0_{-1}^{(j)}$, $j = 1, 2$, *defined in* (29). *Then*

$$\mathcal{F} = \left(\bigcup_{n=0}^{\infty} T^{-n}(\omega_1)\right) \cup \left(\bigcup_{n=0}^{\infty} T^{-n}(\omega_2)\right). \tag{30}$$

where T^{-n} *represents the set of all the preimages of rank-n.*

In order to compute the preimages in (30) let us consider a point $P = (0, p) \in \omega_2$. Its preimages are the real solutions of the algebraic system obtained from (12) with $(q_1', q_2') = (0, p)$:

$$\begin{cases} q_1 \left[1 + v_1(a - c_1) - 2bv_1q_1 - bv_1q_2\right] = 0, \\[2mm] (1 + v_2(a - c_2)) q_2 - 2bv_2q_2^2 - bv_2q_1q_2 = p. \end{cases} \tag{31}$$

From the first of (31) we obtain $q_1 = 0$ or

$$1 + v_1(a - c_1) - 2bv_1q_1 - bv_1q_2 = 0, \tag{32}$$

which means that if the point P has preimages, then they must be located either on the same invariant axis or on the line of (32). With $q_1 = 0$ the second equation becomes a second degree algebraic equation which has two distinct, coincident or no real solutions if the discriminant

$$(1 + v_2 (a - c_2))^2 - 8bv_2 p \tag{33}$$

is positive, zero, or negative, respectively. A similar conclusion holds if (32) is used to eliminate a state variable in the first equation of (31). From this we can deduce that the point P can have no preimages or two preimages on the same axis (which are the same obtained by the restriction (25) of T to the axis q_2) or four preimages, two on the same axis and two on the line of (32). This implies that the set of the rank-1 preimages of the q_2-axis belongs to the same axis and to the line (32). Following the same arguments we can state that the other invariant axis, q_1, has preimages on itself and on the line of equation

$$1 + v_2(a - c_2) - bv_2q_1 - 2bv_2q_2 = 0. \tag{34}$$

It is straightforward to see that the origin $O = (0, 0)$ always has four preimages: $O_{-1}^{(0)} = (0, 0)$, $O_{-1}^{(1)} = (q_1^{o-1}, 0)$, $O_{-1}^{(2)} = (0, q_2^{o-1})$, where q_j^{o-1}, $j = 1, 2$, are given by (39), and

$$O_{-1}^{(3)} = \left(q_1^* + \frac{2v_2 - v_1}{3bv_1v_2}, q_2^* + \frac{2v_1 - v_2}{3bv_1v_2}\right),$$

$$v_1 = 0.24 \quad v_2 = 0.48 \quad c_1 = 3 \quad c_2 = 5 \quad a = 10 \quad b = 0.5$$
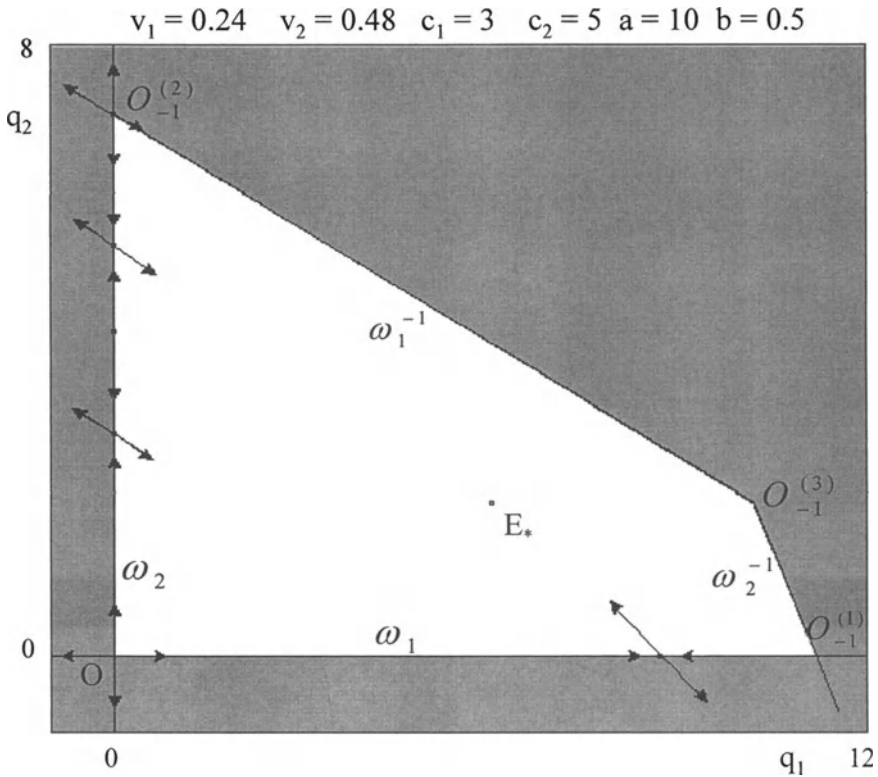
Figure 3: With $c_1 = 3$, $c_2 = 5$, $a = 10$, $b = 0.5$, $v_1 = 0.24$, $v_2 = 0.48$, the boundary of the basin of attraction of the Nash equilibrium E_* is formed by the invariant axes, denoted by ω_1 and ω_2, and their rank-1 preimages ω_1^{-1} and ω_2^{-1}. For this set of parameters the boundary fixed point E_1 is a saddle point with local stable manifold along the q_1-axis, E_2 is a repelling node with a saddle cycle of period two around it, since $v_2 > \frac{2}{a-c_2}$.

located at the intersection of the lines (32) and (34) (see Figure 3). In the situation shown in Figure 3 the segments ω_2 and ω_1 of the coordinate axes, together with their rank-1 preimages, belonging to the lines (32) and (34), and labeled by ω_2^{-1} and ω_1^{-1}, respectively, delimitate the quadrilateral region $OO_{-1}^{(1)} O_{-1}^{(3)} O_{-1}^{(2)}$ of the strategy space (q_1, q_2) which is exactly the basin of attraction of E_*.

These four sides, given by the segments $OO_{-1}^{(1)}$ and $OO_{-1}^{(2)}$ of the coordinate axes and their rank-1 preimages, constitute the whole boundary $\mathcal{F}$ because no preimages of higher rank exist, since ω_{-1}^1 and ω_{-1}^2 belong to the region Z_0 of the plane whose points (q_1', q_2') have no preimages, i.e., the fourth degree algebraic system has no real solutions. This fact can be characterized through the study of the critical curves of the noninvertible map (12) (some basic definitions and

properties of the critical curves are given in Appendix A; see Mira et al. [13], for a more complete treatment).

Since the map T is continuously differentiable, the critical curve LC_{-1} is the locus of points in which the determinant of $J(q_1, q_2)$, given in (17), vanishes, and the critical curve LC, locus of points having two coincident rank-1 preimages, can be obtained as the image, under T, of LC_{-1}(see Appendix A). For the map (12) LC_{-1} is formed by the two branches of an hyperbola, denoted by $LC_{-1}^{(a)}$ and $LC_{-1}^{(b)}$ in Figure 4(a) (its equation is given in Appendix A). Thus also $LC = T(LC_{-1})$ consists of two branches, $LC^{(a)} = T(LC_{-1}^{(a)})$ and $LC^{(b)} = T(LC_{-1}^{(b)})$, represented by the thicker curves of Figure 4(a). These two branches of LC separate the phase plane into three regions, denoted by Z_0, Z_2, and Z_4, whose points have 0, 2, and 4 distinct rank-1 preimages, respectively. It can be noticed that, as already stressed above, the origin always belongs to the region Z_4. It can also be noticed that the line LC_{-1} intersects the axis q_j, $j = 1, 2$, in correspondence of the critical point c_{-1} of the restriction (25) of T to that axis, whose coordinate is given by (36), and that the line LC intersects each axis in correspondence of the critical values of (25), given by (41).

4.2 Contact Bifurcations

In order to understand how complex basin boundaries, like those shown in Figure 2, are obtained, we start from a situation in which $\mathcal{F}$ has a much simpler shape, and then we study the sequence of bifurcations that cause the main qualitative changes in the structure of the basin boundaries as some parameter is varied. Such bifurcations, typical of noninvertible maps, can be characterized by contacts of the basin boundaries with the critical curves (see Mira et al. [13], and references therein).

The simple shape that the frontier $\mathcal{F}$ assumes for values of the parameters like those used in figure 4(a), where the basin of attraction of E_* is a simply connected set, is due to the fact that the preimages of the invariant axes, denoted in Figure 4(a) by ω_i^{-1}, $i = 1, 2$, are entirely included inside the region Z_0, so that no preimages of higher rank exist. The situation is different when the values of the parameters are such that some portions of these lines belong to the regions Z_2 or Z_4. In this case, preimages of higher order of the invariant coordinate axes are obtained, which form new arcs of the frontier $\mathcal{F}$, so that its shape becomes more complex. The switch between these two qualitatively different situations can be obtained by a continuous variation of some parameters of the model, and determines a global (or nonclassical) bifurcation (see Mira et al. [13]). The occurrence of these global bifurcations can be revealed by the study of critical curves. In order to illustrate this, in the rest of this section we fix the marginal costs and the parameters of the demand function at the same values as those used to obtain figures 2, 3, i.e., $c_1 = 3$, $c_2 = 5$, $a = 10$, $b = \frac{1}{2}$, and we vary the values of the speeds of adjustment v_1 and v_2. However, similar bifurcation sequences can be obtained with fixed values of v_1 and v_2 and changing the other parameters. For example,
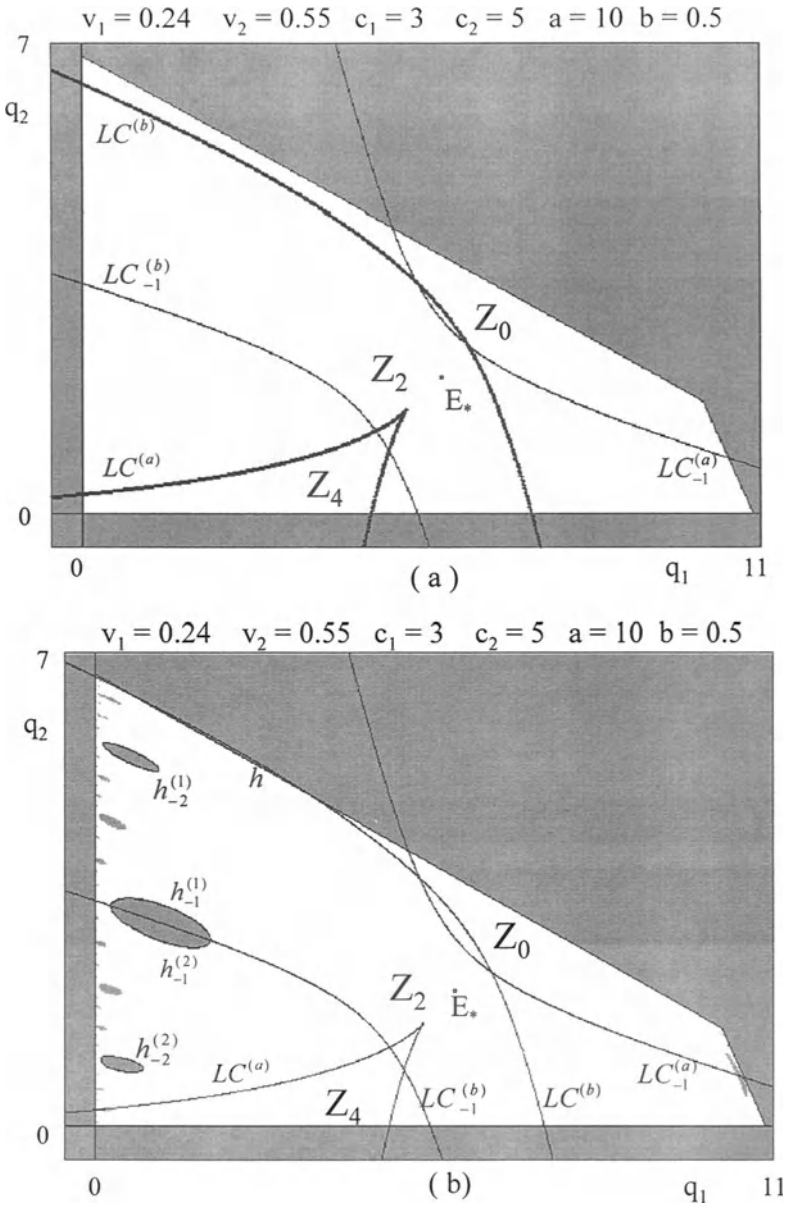
Figure 4: Graphical representation of the basin of attraction of the Nash equilibrium (white region) and the basin $\mathcal{D}(\infty)$ of unbounded trajectories (grey region) together with the basic critical curve LC_{-1}, formed by the two branches of an equilateral hyperbola and the critical curve LC (represented by heavy lines). The values of parameters c_1, c_2, a, b are the same as in Figure 2, whereas in Figure **(a)** $v_1 = 0.24$ and $v_2 = 0.55$, in Figure **(b)** $v_1 = 0.24$ and $v_2 = 0.596$ (just after the contact of LC with ω_1^{-1}).

the same effect of increasing v_1 can be obtained by decreasing the corresponding marginal cost c_1 or by increasing the marginal cost c_2 of the other firm, whereas a simultaneous increase of both v_1 and v_2 is equivalent to a decrease of the parameter a in the demand function.

If, starting from the parameters' values used to obtain the simple basin structure of Figure 4(a), the parameter v_2 is increased, the two branches of the critical curve LC move upward. The first global bifurcation of the basin occurs when the branch of LC, which separates the regions Z_0 and Z_2, becomes tangent to $\mathcal{F}$, that is, to one of the lines (34) or (32). In Figure 4(b) it can be seen that just after the bifurcation value of v_2, at which $LC^{(b)}$ is tangent to the line ω_1^{-1} of (34), a portion of $\mathcal{D}(\infty)$, say H_0 (bounded by the segment h of ω_1^{-1} and LC) that before the bifurcation was in region Z_0, enters into Z_2. The points belonging to H_0 have two distinct preimages, located at opposite sides with respect to the line LC_{-1}, with the exception of the points of the curve $LC^{(b)}$ inside $D(\infty)$ whose preimages, according to the definition of LC, merge on $LC_{-1}^{(b)}$. Since H_0 is part of $\mathcal{D}(\infty)$ its preimages also belong to $\mathcal{D}(\infty)$. The locus of the rank-1 preimages of H_0, bounded by the two preimages of h, is composed by two areas joining along LC_{-1} and forms a *hole* (or lake) of $\mathcal{D}(\infty)$ nested inside $\mathcal{D}(E_*)$. This is the largest hole appearing in Figure 4(b), and is called the *main hole*. It lies entirely inside region Z_2, hence it has two preimages, which are smaller holes bounded by preimages of rank 3 of the q_1-axis. Even these are both inside Z_2. So each of them has two further preimages inside Z_2, and so on. Now the boundary $\mathcal{F}$ is given by the union of an external part, formed by the coordinate axes and their rank-1 preimages (34) and (32), and the boundaries of the holes, which are sets of preimages of higher rank of the q_1-axis. Thus the global bifurcation just described transforms a *simply connected* basin into a *multiply connected* one, with a countable infinity of holes, called an *arborescent sequence of holes*, inside it (see Mira et al. [12] for a rigorous treatment of this type of global bifurcation and Abraham et al. [1] for a simpler and charming exposition).

As v_2 is further increased LC continues to move upward and the holes become larger. This fact causes a sort of predictability loss, since a greater uncertainty is obtained with respect to the destiny of games starting from an initial strategy falling in zone of the holes. If v_2 is further increased a second global bifurcation occurs when LC crosses the q_2-axis at $O_{-1}^{(2)}$. This happens when condition (40) holds, that is, $v_2 = 3/(a - c_2)$, as in Figure 5(a). After this bifurcation all the holes reach the coordinate axis q_2, and the infinite contact zones are the intervals of divergence of the restriction (25), which are located around the critical point (36) and all its preimages under (25) (compare Figure 5(a) with Figure B1(b)). After this bifurcation the basin $\mathcal{D}(E_*)$ becomes simply connected again, but its boundary $\mathcal{F}$ now has a fractal structure, since its shape, formed by infinitely many peninsulas, have a self-similarity property.

The sequence of pictures shown in Figure 5 is obtained with $v_1 = 0.24$ (as in Figure 4) and increasing values of v_2. Along this sequence the point (v_1, v_2)
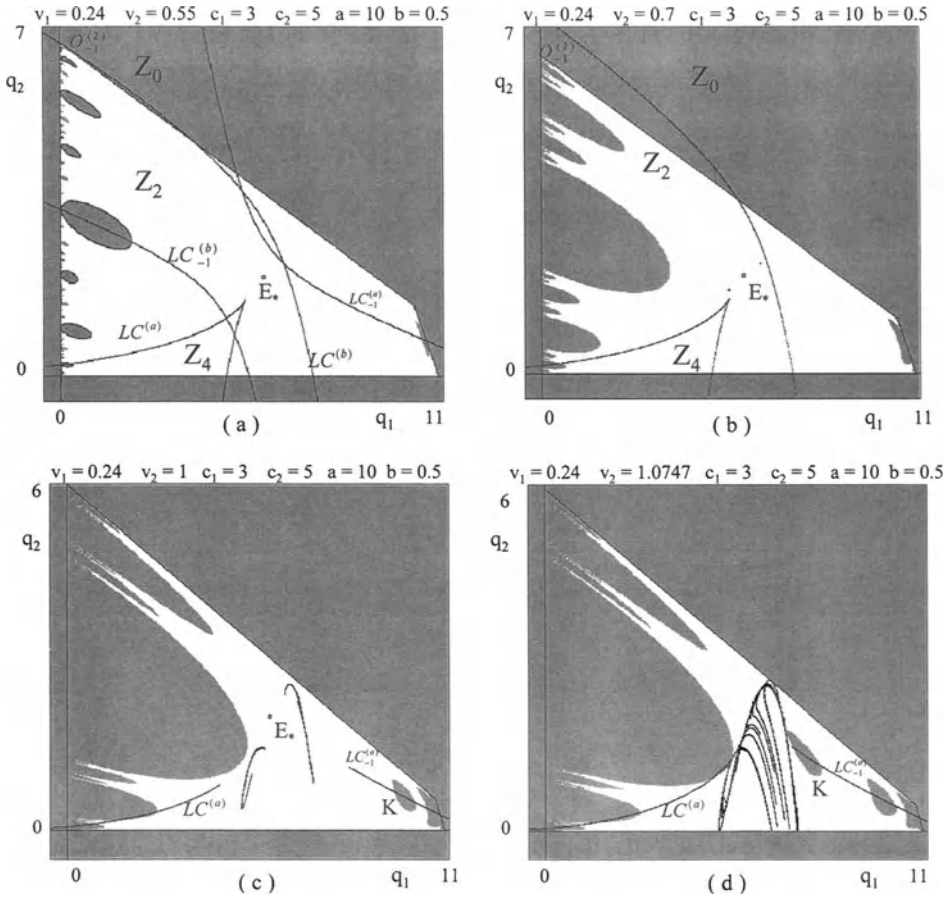
Figure 5: Sequence of numerical simulations of the duopoly map, obtained with fixed parameters $c_1 = 3$, $c_2 = 5$, $a = 10$, $b = 0.5$, $v_1 = 0.24$, and increasing values of v_2.

reaches, in the plane of adjustment speeds, the line of flip bifurcations. When this line is crossed the Nash equilibrium E_* becomes a repelling saddle point, and an attracting cycle of period 2, say C_2, is created near it (as in Figure 5(b)). The flip bifurcation opens a cascade of period doublings, that creates a sequence of attracting cycles of period 2^n followed by the creation of chaotic attractors, which may be cyclic chaotic areas, like the 2-cyclic one shown in Figure 5(c), or a unique chaotic area like that of Figure 5(d).

If v_2 is further increased, new holes, like that denoted by K in Figure 5(c), appear. These are formed by the rank-1 preimages of portions of $\mathcal{D}(\infty)$ which cross $LC^{(a)}$ passing from Z_2 to Z_4, like those evidenced in Figures 5(c,d). Even in this case, the holes are created after contact between LC and $\mathcal{F}$, but, differently

from the hole H_{-1}, the hole K does not generate an arborescent sequence of holes since it has no preimages, belonging entirely to the region Z_0.

In Figure 5(d) the chaotic area collides with the boundary of $\mathcal{D}(\infty)$. This contact bifurcation is known as *final bifurcation* (Mira et al. [13] and Abraham et al. [1]), and causes the destruction of the attractor at finite distance. After this contact bifurcation the generic initial strategy generates an unbounded trajectory, that is, the adjustment process is not able to approach the Nash equilibrium, independently of the initial strategy of the duopoly game.

It is worth noting that, in general, there are no relations between the bifurcations which change the qualitative properties of the basins and those which change the qualitative properties of the attractor at finite distance. In other words, we may have a simple attractor, like a fixed point or a cycle, with a very complex basin structure, or a complex attractor with a simple basin. Both these sequences of bifurcations, obtained by increasing the speeds of adjustment v_i, cause a loss of predictability. After the local bifurcations the myopic duopoly game no longer converges to the global optimal strategy, represented by the Nash equilibrium E_*, and even if the game starts from an initial strategy very close to E_* the duopoly system goes toward a different attractor, which may be periodic or aperiodic. These bifurcations cause, in general, a loss of predictability about the asymptotic behavior of the duopoly system: for example, in the sequence shown in Figure 5 the situation of convergence to the unique Nash equilibrium, as in the static Cournot game, is replaced by asymptotic convergence to a periodic cycle, with predictable output levels, and then by a cyclic behavior with output levels that are not well predictable since the fall inside cyclic chaotic areas and, finally, a situation of erratic behavior, inside a large area of the strategy space, with no apparent periodicity. Instead, the global bifurcations of the basin boundaries cause an increasing uncertainty with respect to the destiny of a duopoly game starting from a given initial strategy, since a small change in the initial condition of the duopoly, or a small exogenous shock during the adjustment process, may cause a great modification to the long-run behavior of the system. Similar bifurcation sequences can also be obtained by increasing the parameter v_1 by a fixed value of v_2. In this case, a contact between LC and ω_2^{-1}, rank-1 preimage of the q_2-axis, gives the first bifurcation that transforms the basin $\mathcal{D}(\mathcal{A})$ from a simply connected into a multiply connected set, with holes near the q_1-axis. Situations with values of v_1 and v_2 both near the critical values $v_i = 3/(a - c_i)$, $i = 1, 2$, can give complex basin boundaries near both the coordinate axes, with two arborescent sequences of holes, generated by contacts of LC with the lines (32) and (34). In any case, the computation of the preimages of the coordinate axes allows us to obtain, according to (30), the exact delimitation of the basin boundary also in these complex situations. For example, in Figure 6 the preimages of the q_1-axis, up to rank-6, are represented for the same set of parameters as that used in Figure 2(b). It can be noticed that some preimages of rank 5 and 6 bound holes that enter the region Z_4, thus giving a faster exponential growth of the number of higher-order preimages. This is the cause for the greater complexity of the basin boundary which is clearly visible in Figure 2(b).
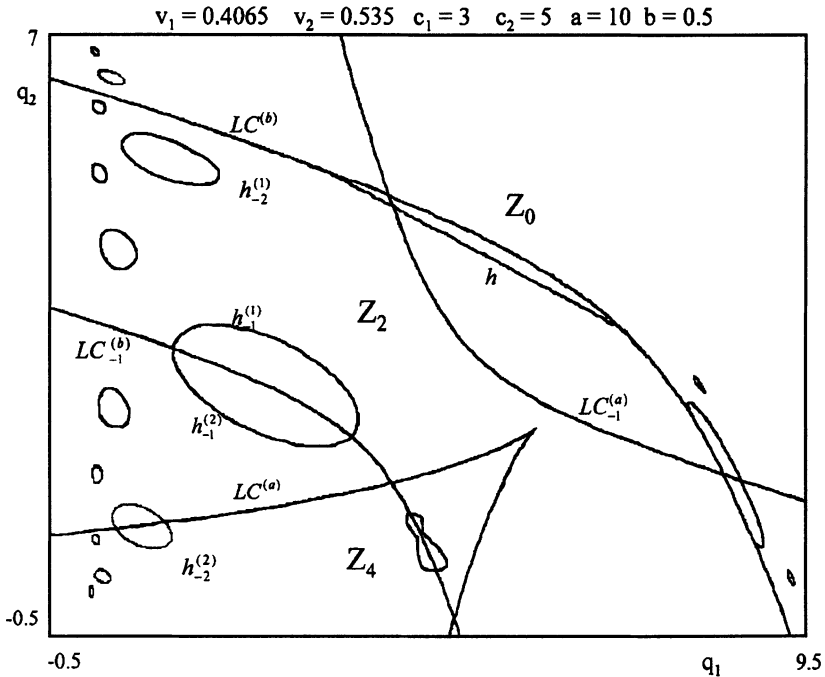
Figure 6: Preimages of the q_1-axis, up to rank 6, obtained with the same set of parameters as those used in Figure 2b.

5 Conclusions

In this paper we have proposed a dynamic Cournot duopoly model where the competing firms do not have a complete knowledge of the demand function. Owing to this lack of information they behave as local (or myopic) profit maximizers, following an adjustment process based on local estimates of marginal profit. If the marginal costs of both producers are not too high, a noncooperative Nash equilibrium exists, and if the behavior of the firms is characterized by relatively low speeds of adjustment such an equilibrium solution is locally asymptotically stable, that is, the local adjustment process converges to the unique Nash equilibrium provided that the duopoly game starts from an initial production strategy inside a well-defined bounded region around the Nash equilibrium.

For higher values of speeds of adjustment the Nash equilibrium becomes unstable and, through period doubling bifurcations, more complex bounded attractors are created around it, which may be periodic cycles or chaotic sets. When the dynamics of the duopoly system become so complicated, the assumption that producers are unable to gain a complete understanding of the structure of the market, and consequently behave myopically, would be even more justified. This adjustment process can also generate unbounded trajectories. Of course, the occurrence of divergent sequences of production strategies is a very unrealistic evolution of the

duopoly game, that simply means that the bounded rationality adjustment mechanism, based on the profit gradients, is completely inadequate to reach optimal, or quasi-optimal, production strategies.

The main result of this paper is the exact determination of the basin of attraction of the attracting sets, wether it be the Nash equilibrium or a more complex attractor around it. This basin of attraction can have a simple shape, but it can also assume, after some global bifurcations, a very complex structure, which causes a sort of indeterminacy about the destiny of the dynamic game starting from a given initial strategy. In general, an increase in the firms' reactivity to profit signals, measured by the speeds of adjustment, can have two different effects on the dynamical properties of the duopoly model. The first one, already studied in the literature, is given by the destabilization of the Nash equilibrium, as discussed above. The second effect, that as far as we know has not yet been studied in the literature, is given by qualitative changes in the structure of the basins of attraction, which can only be revealed by an analysis of the global properties of the nonlinear dynamical system. An exact delimitation of the basin of an attractor of a nonlinear dynamical system is very important in applied models since it gives quantitative information on the possible effects of exogenous shocks of finite amplitude on the evolution of the system. Thus the determination of the global bifurcations, that cause qualitative modifications of the structure of the basins, is important to characterize the robustness of an attractor with respect to external disturbances. In this paper such bifurcations have been studied in detail using critical curves, a relatively new and powerful tool for the study of the global behavior of noninvertible two-dimensional discrete dynamical systems. In the model studied in this paper the main qualitative changes of the global structure of the basins, that for nonlinear maps are generally studied only by numerical methods, can be obtained analytically, through the exact determination of the curves bounding the basin and the knowledge of the critical curves. For this reason the model studied in this paper may also be considered as a pedagogical example for the study of a nonlinear discrete dynamical system of the plane.

Even if in this paper the analysis is limited to the duopoly case with a particular choice of demand and cost functions, we believe that the main conclusions on the attractors and on the structure of their basins of attraction are indicative of what may happen in more general models, and can be seen as a starting point for the study of similar phenomena in oligopoly models with more than two firms and with more general demand and cost functions.

Appendices

A. Critical Curves

In this appendix we give some basic definitions and properties, and a minimal vocabulary, about the theory of noninvertible maps of the plane and the method of

critical curves. We also give the analytical expression of the basic critical curve LC_{-1} of the map (12).

A two-dimensional map can be written in the general form

$$\mathbf{x}' = T(\mathbf{x}) = (g_1(\mathbf{x}), g_2(\mathbf{x})), \tag{35}$$

where $\mathbf{x} = (x_1, x_2) \in \mathbb{R}^2$ is the phase variable, g_1 and g_2 are real valued continuous functions and $\mathbf{x}' = (x'_1, x'_2)$ is called a rank-1 image of $\mathbf{x}$ under T. The point $\mathbf{x}_t = T^t(\mathbf{x})$, $t \in \mathbb{N}$, is called the image (or forward iterate) of rank-t of the point $\mathbf{x}$, and the sequence $\{\mathbf{x}_t\}$ of all these images is the trajectory generated by the initial condition $\mathbf{x}$ (or $\mathbf{x}_0$, since T^0 is identified with the identity map). The fact that the map T is single valued does not imply the existence and uniqueness of its inverse T^{-1}. Indeed, for a given $\mathbf{x}'$ the rank-1 preimage (or backward iterate) $\mathbf{x} = T^{-1}(\mathbf{x}')$ may not exist or it may be multivalued. In such cases T is said to be a noninvertible map. The duopoly model (12) belongs to this class, because if in (12) the point (q_1, q_2) is computed in terms of a given (q'_1, q'_2) a fourth-degree algebraic system is obtained, that can have four, two, or no solutions. As the point (q'_1, q'_2) varies in the plane $\mathbb{R}^2$ the number of solutions, i.e., the number of its real rank-1 preimages, can change. Generally, pairs of real preimages appear or disappear as the point (q'_1, q'_2) crosses the boundary separating regions characterized by a different number of preimages. Such boundaries are characterized by the presence of two coincident (merging) preimages. This leads to the definition of the critical curves, one of the distinguishing features of noninvertible maps. The critical curve of rank-1, denoted by LC, is defined as the locus of points having two, or more, coincident rank-1 preimages, located on a set called LC_{-1}. LC is the two-dimensional generalization of the notion of critical value (local minimum or maximum value) of a one-dimensional map, and LC_{-1} is the generalization of the notion of the critical point (local extremum point). Arcs of LC separate the regions of the plane characterized by a different number of real preimages.

When in (35) g_1 and g_2 are continuously differentiable functions, LC_{-1} is generally given by the locus of points where the Jacobian determinant of T vanishes (i.e., the points where T is not locally invertible):

$$LC_{-1} = \left\{ \mathbf{x} \in \mathbb{R}^2 \mid \det J = 0 \right\},$$

and LC is the rank-1 image of LC_{-1} under T, i.e., $LC = T(LC_{-1})$.

For the map (12) studied in this paper, from the expression of J given in (17), the condition $\det J = 0$ becomes

$$q_1^2 + q_2^2 + 4q_1q_2 - \alpha_1 q_1 - \alpha_2 q_2 + \beta = 0,$$

where

$$\alpha_i = \frac{4(1 + v_j(a - c_j)bv_i) + 1 + v_i(a - c_i)bv_j}{4b^2 v_1 v_2}, \qquad i = 1, 2, \quad j \neq i,$$

and

$$\beta = \frac{(1 + v_1(a - c_1)bv_1)(1 + v_2(a - c_2)bv_2)}{4b^2 v_1 v_2}.$$

This is an hyperbola in the plane (q_1, q_2) with symmetry center in the point $((2\alpha_2 - \alpha_1)/3, (2\alpha_1 - \alpha_2)/3)$ and asymptotes of angular coefficients $\left(-2 \pm \sqrt{3}\right)$. Thus LC_{-1} is formed by two branches, denoted by $LC_{-1}^{(a)}$ and $LC_{-1}^{(b)}$ in Section 4. This implies also that LC is the union of two branches, denoted by $LC^{(a)} = T(LC_{-1}^{(a)})$ and $LC^{(b)} = T(LC_{-1}^{(b)})$. Each branch of the critical curve LC separates the phase plane of T into regions whose points possess the same number of distinct rank-1 preimages. In the case of the map (12) $LC^{(b)}$ separates the region Z_0, whose points have no preimages, from the region Z_2, whose points have two distinct rank-1 preimages, and $LC^{(a)}$ separates the region Z_2 from Z_4, whose points have four distinct preimages. In order to study the action of the multivalued inverse relation T^{-1} it is useful to consider a region Z_k of the phase plane as the superposition of k sheets, each associated with a different inverse. Such a representation is known as *foliation* of the plane (see Mira et al. [13]). Different sheets are connected by folds joining two sheets, and the projections of such folds on the phase plane are arcs of LC. The foliation associated with the map (12) is qualitatively represented in Figure 7. It can be noticed that the cusp point of LC is characterized by three merging preimages at the junction of two folds.

B. Dynamics on the Invariant Axes

In the following we recall some of the properties of the dynamic behavior of the map (25). Such properties are well known since such a map is conjugate to the standard logistic map $x' = \mu x(1 - x)$ through the transformation (27).

The map (25) is a unimodal map with the unique critical point C_{-1} (see Figure 8(a) of coordinate

$$q_j^{C_{-1}} = \frac{1 + v_j(a - c_j)}{4bv_j}, \qquad j = 1, 2, \tag{36}$$

(conjugate to the critical point $x = \frac{1}{2}$ of (26)) and two fixed points O and E_j of coordinates

$$q_j^o = 0, \qquad q_j^{E_j} = \frac{a - c_j}{2b}, \qquad j = 1, 2, \tag{37}$$

(conjugate to the fixed points $x = 0$ and $x = (1 - 1/\mu)$, respectively) corresponding to the boundary fixed points of the duopoly map T. The fixed point O is always repelling for (25), whereas E_j is attracting for $0 < v_j (a - c_j) < 2$. When

$$v_j (a - c_j) = 2 \tag{38}$$

a flip bifurcation occurs which starts the well-known Feigenbaum (or Myrberg) cascade of period doubling bifurcations leading to the chaotic behavior of (25).
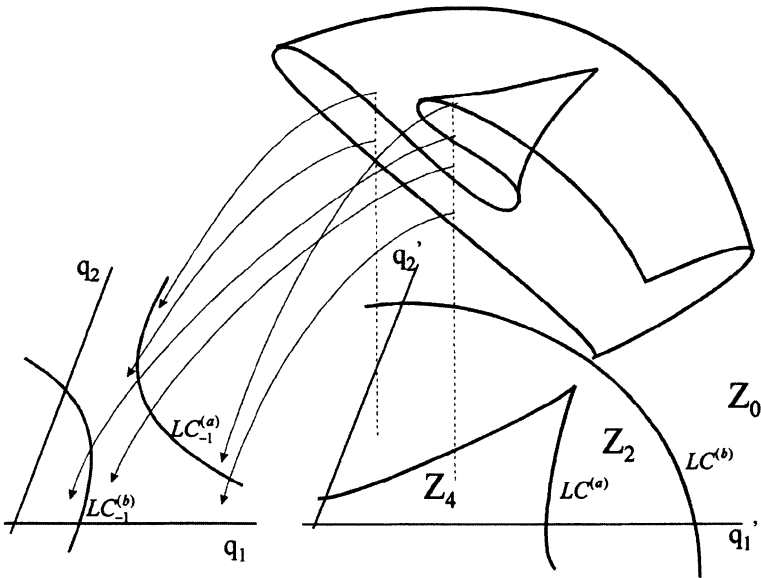
Figure 7: Qualitative graphical representation of the foliation associated with the fourth degree noninvertible map (12). The projections of the folds joining two superimposed sheets are the branches of the critical curve LC. The arrows show the relation between the foliation and the k distinct rank-one preimages of a point belonging to a region Z_k.

Of course, the bifurcation occurring at (38) corresponds to the flip bifurcation of the map T described above, which transforms the saddle point E_j of T into a repelling node. As v_j is further increased, or c_j decreased, cycles of (25) of any order are created: every attracting cycle of (25) corresponds to a saddle cycle of T, located on the line $q_i = 0$, with the attracting branch along the invariant axis, and every repelling cycle of (25) corresponds to a repelling node cycle for T. For any given value of $v_j(a - c_j) \in (2, 3)$ we can have only one attractor, that may be a cycle or a cyclic-invariant chaotic interval (as for the standard logistic (26) with $\mu \in (3, 4)$) whose basin of attraction is bounded by the unstable fixed point O and its preimage O_{-1}^j, of coordinate

$$q_j^{o-1} = \frac{1 + v_j(a - c_j)}{2bv_j} \tag{39}$$

(conjugate to the point $x = 1$ of the standard logistic). Any trajectory of (25) starting from an initial point taken out of the interval $\left[0, q_j^{o-1}\right]$ is divergent toward $-\infty$. At

$$v_j(a - c_j) = 3 \tag{40}$$

the whole interval $\left[0, q_j^{o-1}\right]$ is an invariant chaotic interval. For $v_j(a - c_j) > 3$, as in Figure 8(b), the generic trajectory of (25) is divergent (see, e.g., Devaney, [4,
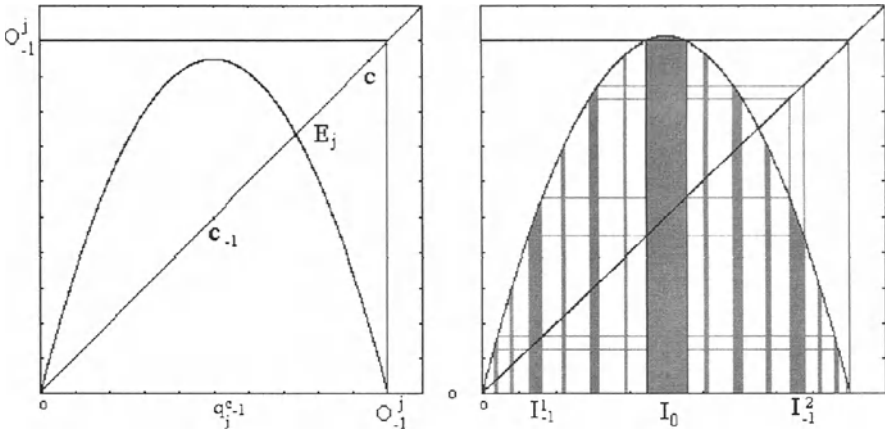
Figure 8: Graph of the map (25), conjugate to the logistic map (26). In **(a)** $v_j(a - c_j) < 3$. In this case $q_j^c < q_j^{o-1}$; hence all points inside $I = \left[0, q_j^{o-1}\right]$ remain inside I under iteration of (25). In **(b)** $v_j(a - c_j) > 3$. In this case $q_j^c > q_j^{o-1}$ and an interval I_0 exists around q_j^c whose points have images out of I, so that their trajectories are divergent. The preimages of I_0 are two smaller intervals, denoted in figure by I_{-1}^1 and I_{-1}^2, whose points escape interval I after two iterations; these two intervals have four intervals as preimages, etc. The union of all the preimages, of any rank, of I_0, is an open and dense set on I whose points generate unbounded and negative trajectories. Its complement in I has zero measure and is homeomorphic to a Cantor set.

p. 34]). This final bifurcation occurring when (40) holds, is characterized by the collision (or merging) of the critical value c, whose coordinate

$$q_j^C = \frac{\left[1 + v_j(a - c_j)\right]^2}{8bv_j} \tag{41}$$

is given by the image of the critical point c_{-1}, with the basin boundary at q_j^{o-1}. In fact, $q_j^{o-1} = q_j^C = 4/2bv_j$ when (40) holds.

Acknowledgments

REFERENCES

[1] Abraham, R., L. Gardini, and C. Mira. *Chaos in Discrete Dynamical Systems (A Visual Introduction in Two Dimensions)*. Springer-Verlag, New York, 1996.

[2] Bonanno, G. Oligopoly Equilibria When Firms Have Local Knowledge of Demand. *International Economic Review*, **29**, 45–55, 1988.

[3] Bonanno, G. and C. Zeeman. Limited Knowledge of Demand and Oligopoly Equilibria. *Journal of Economic Theory*, **35**, 276–283, 1985.

[4] Devaney, R. L. *An Introduction to Chaotic Dynamical Systems*. Benjamin/Cummings, Menlo Park, CA, 1987.

[5] Dixit, A. Comparative Statics for Oligopoly. *International Economic Review*, **27**, 107–122, 1986.

[6] Fisher, F. M. The Stability of the Cournot Oligopoly Solution: The Effect of Speeds of Adjustment and Increasing Marginal Costs. *Review of Economic Studies*, **28**, 125–135, 1961.

[7] Flam, S. D. Oligopolistic Competition: From Stability to Chaos. In: F. Gori, L. Geronazzo and M. Galeotti (eds.), *Nonlinear Dynamics in Economics and Social Sciences*. Lecture Notes in Economics and Mathematical Systems, vol. 399. pp. 232–237, Springer-Verlag, Berlin, 1993.

[8] Furth, D. Stability and Instability in Oligopoly. *Journal of Economic Theory*, **40**, 197–228, 1986.

[9] Gumowski, I. and C. Mira. *Dynamique Chaotique*. Cepadues Editions, Toulose, 1980.

[10] Hahn, F. The Stability of the Cournot Oligopoly Solution. *Review of Economic Studies*, **29**, 329–331, 1962.

[11] McManus, M. and R. E. Quandt. Comments on the Stability of the Cournot Oligopoly Model. *Review of Economic Studies*, **27**, 136–139, 1961.

[12] Mira, C., L. Gardini, A. Barugola, and J. C. Cathala. *Chaotic Dynamics in Two-Dimensional Noninvertible Maps*. World Scientific, Singapore, 1996.

[13] Mira, C., D. Fournier-Prunaret, L. Gardini, H. Kawakami, and J. C. Cathala. Basin Bifurcations of Two-Dimensional Noninvertible Maps: Fractalization of Basins. *International Journal of Bifurcations and Chaos*, **4**, 343–381, 1994.

[14] Mira, C. and C. Rauzy. Fractal Aggregation of Basin Islands in Two-Dimensional Quadratic Noninvertible Maps. *International Journal of Bifurcations and Chaos*, **5**, 991–1019, 1995.

[15] Okuguchi, K. Adaptive Expectations in an Oligopoly Model. *Review of Economic Studies*, **37**, 233–237, 1970.

[16] Sacco, P. L. Adaptive Response and Cournotian Behavior. *Economic Notes*, **20**, 474–496, 1991.

[17] Rosen, J. B. Existence and Uniqueness of Equilibrium Points for Concave *n*-Person Games. *Econometrica*, **33**, 520–534, 1965.

[18] Teocharis, R. D. On the Stability of the Cournot Solution of the Oligopoly Problem. *Review of Economic Studies*, **27**, 133–134, 1960.

[19] Varian, H. R. *Microeconomic Analysis*, 3rd ed. W. W. Norton, 1992.